Influence of spatial distribution and the type of material on the occurrence of bandgaps in phononic crystals

Sebastian GARUS[1] *, Wojciech SOCHACKI[1], Paweł KWIATOŃ[1], Marcin NABIAŁEK[2], Jana PETRŮ[3], and Mariusz KUBANEK[4]

[1] Faculty of Mechanical Engineering and Computer Science, Department of Mechanics and Fundamentals of Machinery Design, Czestochowa University of Technology, Dąbrowskiego 73, 42-201 Częstochowa, Poland

[2] Faculty of Production Engineering and Materials Technology, Department of Physics, Czestochowa University of Technology, Armii Krajowej 19, 42-201 Częstochowa, Poland

[3] Department of Machining, Assembly and Engineering Metrology, Faculty of Mechanical Engineering, VSB-Technical University of Ostrava, 70833 Ostrava, Czech Republic

[4] Faculty of Mechanical Engineering and Computer Science, Department of Computer Science, Czestochowa University of Technology, Dąbrowskiego 73, 42-201 Częstochowa, Poland

Abstract. The study investigated the effect of the fill factor, lattice constant, and the shape and type of meta-atom material on the reduction of mechanical wave transmission in quasi-two-dimensional phononic structures. A finite difference algorithm in the time domain was used for the analysis, and the obtained time series were converted into the frequency domain using the discrete Fourier transform. The use of materials with large differences in acoustic impedance allowed to determine the influence of the meta-atom material on the propagation of the mechanical wave.

Key words: finite difference time domain; band gap; phononic crystal; mechanical waves; propagation.

1. INTRODUCTION

The first works on wave propagation in periodic structures appeared at the end of the 19th century [1], and since then more and more complicated structures have been studied [2]. Phenomena related to the periodicity of systems occur not only for mechanical waves [3] but also for electromagnetic [4], plasmonic [5] and thermal ones [6]. The most interesting, non-naturally occurring phenomena related to the ordered structure include invisibility [7], imaging below wavelength [8], or wave bending in the "wrong" direction [9]. Structures that scatter mechanical waves are called phononic structures [10], while those that scatter electromagnetic waves are called photonic structures [11]. In these structures, the size of meta-atoms is comparable to the wavelength, therefore the interference on meta-atoms (individual elements of an artificial structure) is quite important and has a significant impact on wave propagation. In this work, phononic structures are analyzed.

The phenomenon where the mechanical wave with the given frequencies does not propagate in the structure is called the occurrence of a phononic band gap (PhnBG) [12, 13]. By designing the distribution of the material in the structure so that there are band gaps in the given regions, it is possible to manage the

propagation of mechanical waves, and thus to design devices such as, for example, selective filters [14], acoustic filters [15], acoustic cloaking [16], medical devices [17], waveguides [18], mechanical wave lenses [19], acoustic diodes [20], acoustic barriers [21] as well as energy harvesting devices [22–24].

More and more work is focused on obtaining a bandgap with appropriate properties. In [25] the authors try to suppress waves of a given frequency range. On the other hand, in [26] the authors tried to obtain the broadest possible band gap. Similarly, in works [27–29] the authors, using the genetic algorithm, minimized the transmissions in the range of acoustic waves. In [30] the reflectance coefficient was maximized to reflect the largest possible range of mechanical wave energies. The influence of layer thickness on transmission in one-dimensional structures made of amorphous materials was also analyzed [31]. The occurrence of numerical and experimental gaps has been demonstrated in [32]. Much of the work related to phononic crystals focuses on topology optimization [33–37].

Wave propagation and determination of band gaps are possible with the use of a large number of numerical methods. These include the plane wave expansion method (PWE) [38], one-dimensional transmission line model (TLM) [39], transfer matrix method (TMM) [40, 41], multiple scattering theory (MST) [42], finite element method (FEM) [43–45], boundary element method (BEM) [46, 47] and the finite difference time domain (FDTD) [48, 49].

The aim of the work was to determine how the propagation

*e-mail: sebastian.garus@pcz.pl

S. Garus, W. Sochacki, P. Kwiatoń, M. Nabiałek, J. Petrů, and M. Kubanek

of a mechanical wave in quasi-two-dimensional phononic structures is influenced by the fill factor, lattice constant and the shape and type of material from which meta-atoms are made.

2. FINITE DIFFERENCE TIME DOMAIN

The finite difference time domain algorithm was used to analyze propagation of the mechanical wave in phononic structures. The system of differential equations describes the propagation of a mechanical wave:

$$\frac{1}{\rho c^2}\frac{\partial p(\vec{x},t)}{\partial t} = -\nabla \cdot \vec{v}(\vec{x},t),$$
$$\rho \frac{\partial \vec{v}(\vec{x},t)}{\partial t} = -\nabla p(\vec{x},t), \tag{1}$$

where the vector velocity field is $\vec{v}(\vec{x},t)$ and the pressure field is $p(\vec{x},t)$. The density and phase velocity of the material are ρ and c, respectively. Appropriate transformations to two-dimensional space and in the notation typical for the FDTD algorithm (subscripts define the place in space and the upper ones in time) give the following system of equations:

$$p\big|_{i,j}^{t+1} = p\big|_{i,j}^{t} - \rho\big|_{i,j}\left(c\big|_{i,j}\right)^2 \cdot \frac{\Delta t}{\Delta z}\left(\begin{array}{c} v_x\big|_{i,j}^{t+\frac{1}{2}} - v_x\big|_{i-1,j}^{t+\frac{1}{2}} \\ + v_y\big|_{i,j}^{t+\frac{1}{2}} - v_y\big|_{i,j-1}^{t+\frac{1}{2}} \end{array}\right),$$

$$v_x\big|_{i,j}^{t+\frac{1}{2}} = v_x\big|_{i,j}^{t-\frac{1}{2}} - \frac{\Delta t}{\rho\big|_{i,j}\Delta z}\left(p\big|_{i+1,j}^{t} - p\big|_{i,j}^{t}\right), \tag{2}$$

$$v_y\big|_{i,j}^{t+\frac{1}{2}} = v_y\big|_{i,j}^{t-\frac{1}{2}} - \frac{\Delta t}{\rho\big|_{i,j}\Delta z}\left(p\big|_{i,j+1}^{t} - p\big|_{i,j}^{t}\right).$$

The simulated area was 0.36 m by 1.06 m. Gaussian impulse was used as the soft wave source. Around the simulation area, there was a four-centimeter PML layer, in which the propagating mechanical wave was quenched.

Table 1 summarizes the initialization parameters of the FDTD algorithm used, which include the maximum and minimum speed of mechanical wave propagation in the simulation, respectively c_{max} and c_{min}, minimum wavelength λ_{min}, steps in space and simulation time, respectively Δz and Δt, the upper range of acoustic frequencies f_{max} and minimum the propagating wavelength λ_{min}. The step in time Δt was determined based on the step in space Δz from the Courant stability condition. Moreover, Table 1 summarizes the parameters of the materials used, such as density ρ and the speed of propagation of mechanical waves c. Material A was air, B is PLA (polylactic acid), W is water, and AA is the $Zr_{55}Cu_{30}Ni_5Al_{10}$ amorphous alloy.

The pressure field distribution after 15 000 time steps is shown in Fig. 1. The obtained time series of pressure values at measurement points P1 (between the source and the structure) and P2 (behind the structure) are shown in Fig. 2. It should be noted that the simulation stabilizes after 9 000 steps. The power spectra determined are presented in Fig. 3. The wave transmission determined for the presented structure was 20.2%.
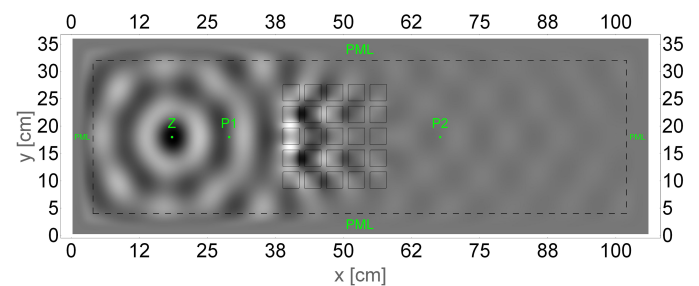

Fig. 1. Pressure distribution over 15 000 time steps for a soft sine wave source of 4143 kHz
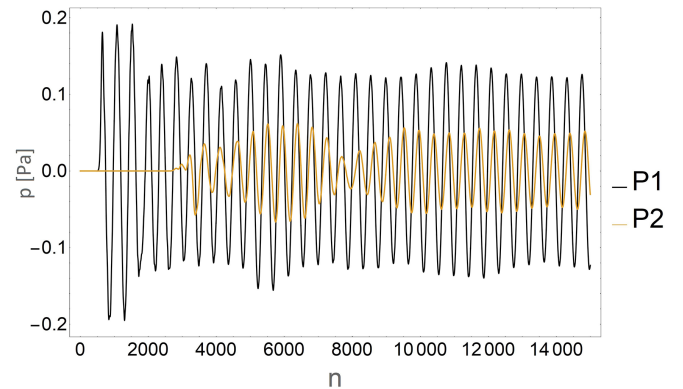

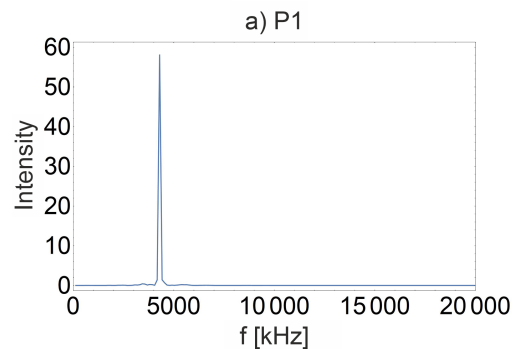**Fig. 2.** Time series of pressure values at measuring points P1 and P2 for a sinusoidal source

Table 1
FDTD algorithm and material parameters [50–52]

Parameter	Value	Parameter	Value
c_{max}	2300 m/s	c_A	331.45 m/s
c_{min}	330 m/s	ρ_B	1240 kg/m^3
f_{max}	4 kHz	c_B	2220 m/s
λ_{min}	8.25 cm	ρ_W	1000 kg/m^3
Δz	2.5 mm	c_W	1500 m/s
Δt	$5.43 \cdot 10^{-7}$ s	ρ_{AA}	6829 kg/m^3
ρ_A	1.29 kg/m^3	c_{AA}	1633 m/s

Fig. 3a

2

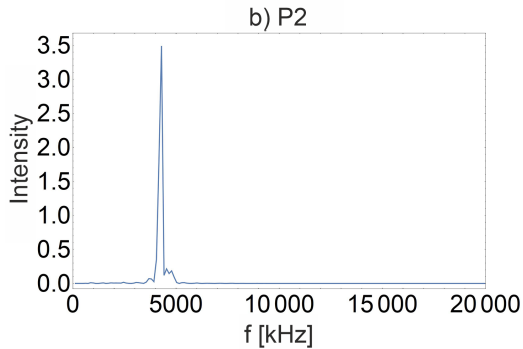*Bull. Pol. Acad. Sci. Tech. Sci.*, vol. 71, no. 3, e144609, 2023

Fig. 3. Time series of pressure values at measuring points P1 and P2 for a sinusoidal source

3. INFLUENCE OF THE FILL FACTOR ON THE PROPAGATION OF A MECHANICAL WAVE

To investigate the effect of the fill factor of the unit cell on the propagation and transmission of the mechanical wave, a simulation of the Gaussian impulse was performed for 5 000 time steps. A 25-element structure with a regular cubic system for a lattice constant of 4 cm was analyzed. Square meta-atoms with sides of 1 cm, 1.5 cm, 2 cm, and 2.5 cm were used, which gave unit cell fill factors of 6%, 14%, 25% and 39%, respectively.

Figures 4a–d show the spatial distribution of pressure after 5 000 time steps for selected values of the unit cell filling factor. With the fill factors at the level of 6% and 14% (Fig. 4a and Fig. 4b), there were no local inter-meta-atomic maximums, which were observed for the fill factors of 25% and 39% (Fig. 4c and Fig. 4d). Figures 4e–h show the signal power spectra for the P2 point for different unit cell filling factors. For the duty cycle of 6% (Fig. 4e), there was a narrow low transmission band for frequencies around 4 kHz, which, with increasing the duty cycle to 14% (Fig. 4f) and then up to 25% (Fig. 4g), slightly increased its width. Increasing the value of the duty cycle to 39% (Fig. 4h) resulted in the formation of a wide band in the frequency range between 2 kHz and 4 kHz. Increasing the geometry of meta-atoms resulted in the occurrence of local areas of increased pressure in the inter-meta-atomic zone (Fig. 4c

and Fig. 4d), thus increasing the frequency range of the low-energy mechanical wave band (Fig. 4g and Fig. 4h).

4. EFFECT OF LATTICE CONSTANT ON MECHANICAL WAVE PROPAGATION

The study of the effect of the lattice constant for a structure with a regular cubic system with meta-atoms with a square cross-section of 1.5 cm was carried out for the interatomic distances of 2 cm, 2.5 cm, 3 cm and 3.5 cm (Fig. 5a–h).

Figures 5a–d show the pressure distributions for structures with the tested lattice constants after 5 000 time steps. The local areas of increased pressure were characterized by low amplitude values. As can be seen in Figs. 5e–h, where the power spectra for the time series in point P2 are presented, the increase in the lattice constant from 2 cm (Fig. 5e) to 2.5 cm (Fig. 5f), and then to 3 cm (Fig. 5g) resulted in significant reductions in the intensity of the peaks in the power spectrum. As a result of increasing the lattice constant to 3 cm (Fig. 5h), a low-intensity band was created in the frequency range from 4 kHz to 5.2 kHz.

5. THE INFLUENCE OF THE CROSS-SECTION SHAPE AND THE MATERIAL OF META-ATOMS ON THE PROPAGATION OF A MECHANICAL WAVE

By examining the influence of the shape of meta-atoms on wave propagation, an analysis of mechanical wave propagation in structures built of meta-atoms with cross-sections in the shape of a circle, square and triangle was carried out. The projection length of each shape along the horizontal axis was 2.5 cm and the lattice constant was 3.5 cm. The analysis was performed for 5 000 Gaussian pulse propagation time steps. Figures 6a–c show the pressure distribution of the analyzed area for structures composed of meta-atoms with different cross-sections.

In all cases, the formation of local areas of increased pressure amplitudes was observed, which was related to the mutual relation between the value of the lattice constant and the duty cycle. The power spectra are shown in Figs. 6d–f. The analysis of the results presented in Fig. 6 leads to the conclusion
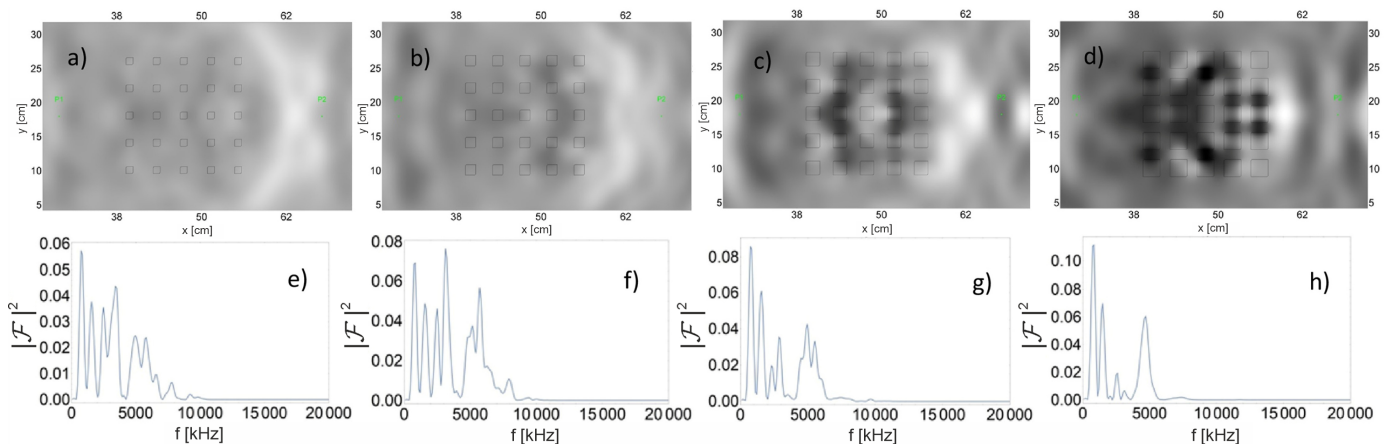

Fig. 4. Pressure distribution for the fill factor of the unit cell at the level of a) 6%, b) 14%, c) 25%, d) 45%, and the corresponding power spectrum e) 6%, f) 14%, g) 25%, h) 45%
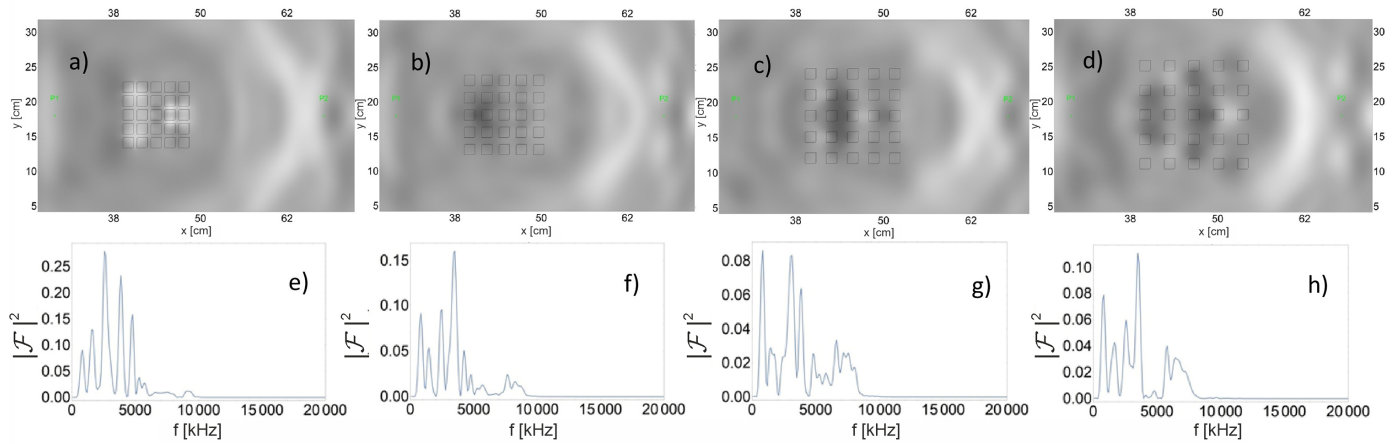
Fig. 5. Pressure distribution for a lattice constant equal to a) 2 cm, b) 2.5 cm, c) 3 cm, d) 3.5 cm, and the corresponding power spectra e) 2 cm, f) 2.5 cm, g) 3 cm, h) 3.5 cm
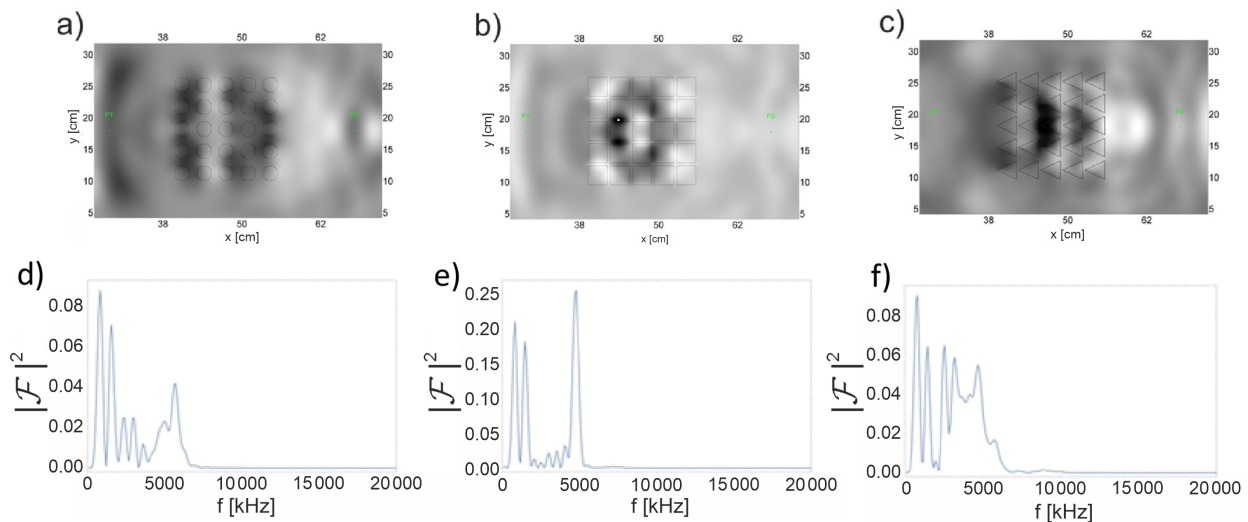

Fig. 6. Pressure distribution for meta-atoms with a cross-section in the shape of a) circle, b) square, c) triangle, and the corresponding signal power spectra for meta-atoms with a cross-section in the shape of d) circle, e) square, f) triangle

that for the round (Fig. 6d) and triangular (Fig. 6f) meta-atoms, power spectra of lower intensity than in the case of square meta-atoms (Fig. 6e) were obtained. The use of square meta-atoms produces a limited spectrum range of low intensity. The use of circular meta-atoms, apart from lowering the value of the power spectrum in the entire analyzed frequency range, also leads to the creation of a wider area of very low intensity. It can therefore be concluded that the circular cross-section of meta-atoms is the most advantageous one for minimizing the energy of mechanical waves. To investigate the effect of the type of meta-atom material on the propagation of the Gaussian impulse, an analysis was carried out for elements made of PLA, the $Zr_{55}Cu_{30}Ni_5Al_{10}$ amorphous alloy and a thin-walled one-sided closed pipe made of PLA filled with water.

Structures composed of meta-atoms with a circular cross-section 2.5 cm in diameter and a lattice constant of 3.5 cm were analyzed. 5 000 algorithm time steps were performed for each case. Figure 7a shows the pressure time series at point P2 for

structures made of PLA, thin-walled elements filled with water and for those made of the $Zr_{55}Cu_{30}Ni_5Al_{10}$ amorphous alloy.

Then, Fig. 7b shows a graph of the differences in pressure values between the series for PLA and the time series at point P2 for the runs where the structure was made of thin-walled elements filled with water and for the case where the structure was made of the $Zr_{55}Cu_{30}Ni_5Al_{10}$ amorphous alloy. Based on the obtained waveforms, power spectra were obtained (Fig. 8a) for the time series from Fig. 7a, and Fig. 8d shows a graph of differences between the values of the power spectrum for the structure made of PLA from Fig. 8a, and the values of power spectra for structures made of thin-walled elements filled with water or made of the $Zr_{55}Cu_{30}Ni_5Al_{10}$ amorphous alloy. The differences presented result from different acoustic impedances of meta-atoms for the examined structures. The differences presented in Figs. 7b and 8b are two orders of magnitude smaller than the curves shown in Figs. 7a and 8a. This leads to the conclusion that in the analyzed practical applications, the choice of one

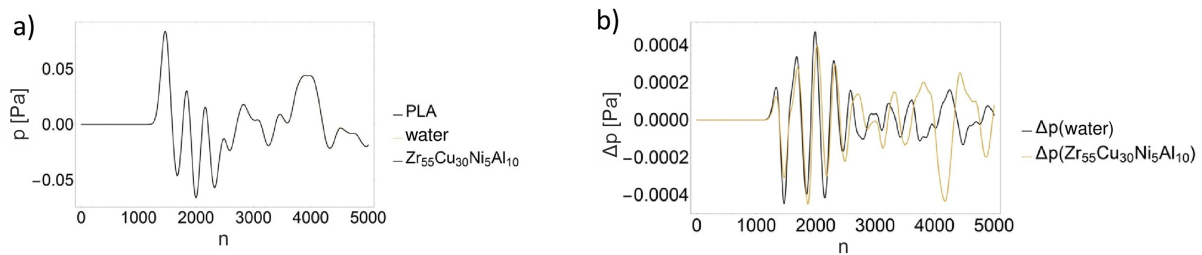Influence of spatial distribution and the type of material on the occurrence of bandgaps in phononic crystals

Fig. 7. a) Pressure time series at point P2 for structures composed of PLA, thin-walled elements filled with water and for those made of $Zr_{55}Cu_{30}Ni_5Al_{10}$ amorphous alloy; b) Differences in time series from point P2 between the structure made of PLA and made of thin-walled elements filled with water or of the $Zr_{55}Cu_{30}Ni_5Al_{10}$ amorphous alloy
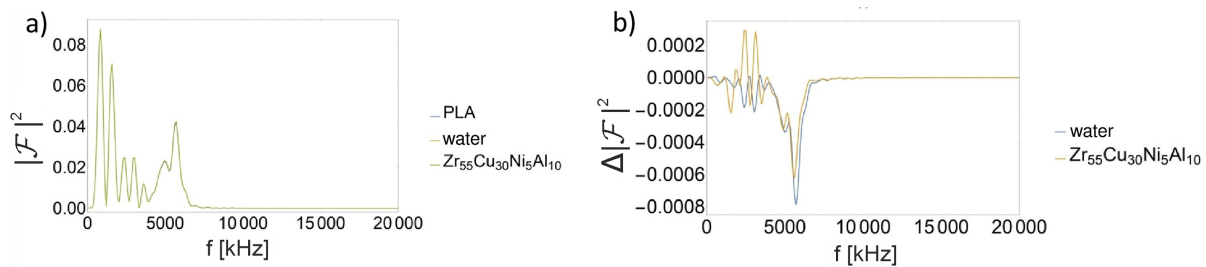
Fig. 8. a) Signal power spectra at the measurement point P2 for the structure made of PLA, thin-walled elements filled with water and for those made of the $Zr_{55}Cu_{30}Ni_5Al_{10}$ amorphous alloy; b) Differences in the power spectra from point P2 between the structure made of PLA and the structure made of thin-walled elements filled with water or of the $Zr_{55}Cu_{30}Ni_5Al_{10}$ amorphous alloy

of the materials with a significantly higher acoustic impedance than the surroundings should be dictated primarily by economic considerations.

6. CONCLUSIONS

The analysis of mechanical wave propagation was carried out using the FDTD algorithm, and the power spectra were obtained from the results of the discrete Fourier transform of time series pressure changes at selected measurement points. As part of the research conducted, the presence of local areas of increased pressure amplitude of the propagating mechanical wave in the inter-meta-atomic spaces inside the phononic structure, which caused a reduction in the amplitude of selected frequency ranges of the mechanical wave transmitted through the structure, was demonstrated. The analysis of the power spectrum made it possible to determine the transmission value for a given frequency. The meta-atom base cell fill factor above 39% in the analyzed structures resulted in the formation of a wide low-intensity band in the frequency range from 2 kHz to 4 kHz. Local areas of increased pressure amplitude in the inter-meta-atomic zone occurred for structures with a higher value of the fill factor, which resulted in the widening of the low wave intensity band. Increasing the lattice constant decreased the intensity of the propagating wave, while the lowest intensity band (in the frequency range from 4 kHz to 5.2 kHz) was obtained for the lattice constant equal to 3 cm. The analysis conducted showed that the structures composed of round and triangular meta-atoms were characterized by power spectra of lower intensity than in the case of square meta-atoms. The use of square meta-atoms resulted in a limited spectrum range of low intensity. The use of circular meta-atoms, apart from lowering the value of the power spectrum in the entire analyzed frequency range, also led to the creation of a wider area of very low intensity. The structure composed of meta-atoms with a circular cross-section turned out to be the most advantageous one for minimizing the energy of mechanical waves. The difference in acoustic impedance between the disturbance propagation center and the meta-atom material was so large that the change of material did not significantly affect wave propagation and its spectrum.

REFERENCES
[1] Lord Rayleigh, 'XVII. "On the maintenance of vibrations by forces of double frequency, and on the propagation of waves through a medium endowed with a periodic structure," *Philos. Mag.*, vol. 24, no. 147, pp. 145–159, 1887, doi: 10.1080/14786448708628074.

Bull. Pol. Acad. Sci. Tech. Sci., vol. 71, no. 3, p. e144609, 2023

5

S. Garus, W. Sochacki, P. Kwiatoń, M. Nabiałek, J. Petrů, and M. Kubanek

[2] P.A. Martin, *Multiple scattering: interaction of time-harmonic waves with N obstacles*. Cambridge: Cambridge University Press, 2006.

[3] J. Li and C.T. Chan, "Double-negative acoustic metamaterial," *Phys. Rev. E*, vol. 70, no. 5, p. 055602, 2004, doi: 10.1103/PhysRevE.70.055602.

[4] D.R. Smith, J.B. Pendry, and M.C.K. Wiltshire, "Metamaterials and negative refractive index," *Science*, vol. 305, no. 5685, pp. 788–792, 2004, doi: 10.1126/science.1096796.

[5] F.J. Garcia-Vidal, L. Martín-Moreno, and J.B. Pendry, "Surfaces with holes in them: new plasmonic metamaterials," *J. Opt. A: Pure Appl. Opt.*, vol. 7, no. 2, pp. S97–S101, 2005, doi: 10.1088/1464-4258/7/2/013.

[6] M. Maksimović and Z. Jakšić, "Modification of thermal radiation by periodical structures containing negative refractive index metamaterials," *Phys. Lett. A*, vol. 342, no. 5–6, pp. 497–503, 2005, doi: 10.1016/j.physleta.2005.05.076.

[7] T.-H. Chen, B. Zheng, C. Qian, and H.-S. Chen, "Progress of novel electromagnetic cloaking research," *Acta Phys. Sin.*, vol. 69, no. 15, p. 154104, 2020, doi: 10.7498/aps.69.20200976.

[8] A. Grbic and G.V. Eleftheriades, "Overcoming the Diffraction Limit with a Planar Left-Handed Transmission-Line Lens," *Phys. Rev. Lett.*, vol. 92, no. 11, p. 117403, 2004, doi: 10.1103/PhysRevLett.92.117403.

[9] J. Pendry, "Negative refraction," *Contemporary Physics*, vol. 45, no. 3, pp. 191–202, 2004, doi: 10.1080/00107510410001667434.

[10] A. Sukhovich, L. Jing, and J.H. Page, "Negative refraction and focusing of ultrasound in two-dimensional phononic crystals," *Phys. Rev. B*, vol. 77, no. 1, p. 014301, 2008, doi: 10.1103/PhysRevB.77.014301.

[11] S. Foteinopoulou and C.M. Soukoulis, "Electromagnetic wave propagation in two-dimensional photonic crystals: A study of anomalous refractive effects," *Phys. Rev. B*, vol. 72, no. 16, p. 165112, 2005, doi: 10.1103/PhysRevB.72.165112.

[12] J. Wang, G. Dai, and J. Huang, "Thermal Metamaterial: Fundamental, Application, and Outlook," *iScience*, vol. 23, no. 10, p. 101637, 2020, doi: 10.1016/j.isci.2020.101637.

[13] S. Garus, W. Sochacki, M. Kubanek, and M. Nabiałek, "Minimizing the number of layers of the quasi-one-dimensional phononic structures," *Bull. Pol. Acad. Sci. Tech. Sci.*, vol. 70, no. 1, p. e139394, 2022, doi: 10.24425/bpasts.2021.139394.

[14] X. Zhang, Y. Li, Y. Wang, Z. Jia, and Y. Luo, "Narrow-band filter design of phononic crystals with periodic point defects via topology optimization," *Int. J. Mech. Sci*, vol. 212, p. 106829, 2021, doi: 10.1016/j.ijmecsci.2021.106829.

[15] C.J. Rupp, M.L. Dunn, and K. Maute, "Switchable phononic wave filtering, guiding, harvesting, and actuating in polarization-patterned piezoelectric solids," *Appl. Phys. Lett.*, vol. 96, no. 11, p. 111902, 2010, doi: 10.1063/1.3341197.

[16] L. Pomot, C. Payan, M. Remillieux, and S. Guenneau, "Acoustic cloaking: Geometric transform, homogenization and a genetic algorithm," *Wave Motion*, vol. 92, p. 102413, 2020, doi: 10.1016/j.wavemoti.2019.102413.

[17] R.H. Olsson, I.F. El-Kady, M.F. Su, M.R. Tuck, and J.G. Fleming, "Microfabricated VHF acoustic crystals and waveguides," *Sens. Actuator A Phys.*, vol. 145–146, pp. 87–93, 2008, doi: 10.1016/j.sna.2007.10.081.

[18] B. Morvan *et al.*, "Ultra-directional source of longitudinal acoustic waves based on a two-dimensional solid/solid phononic crystal," *J. Appl. Phys.*, vol. 116, no. 21, p. 214901, 2014, doi: 10.1063/1.4903076.

[19] S. Huang, L. Peng, H. Sun, Q. Wang, W. Zhao, and S. Wang, "Frequency response of an underwater acoustic focusing composite lens," *Appl. Acoust.*, vol. 173, p. 107692, 2021, doi: 10.1016/j.apacoust.2020.107692.

[20] X.-F. Li, X. Ni, L. Feng, M.-H. Lu, C. He, and Y.-F. Chen, "Tunable unidirectional sound propagation through a sonic-crystal-based acoustic diode," *Phys. Rev. Lett.*, vol. 106, no. 8, p. 084301, 2011, doi: 10.1103/PhysRevLett.106.084301.

[21] J.V. Sanchez-Perez, C. Rubio, R. Martinez-Sala, R. Sanchez-Grandia, and V. Gomez, "Acoustic barriers based on periodic arrays of scatterers," *Appl. Phys.Lett.*, vol. 81, no. 27, pp. 5240–5242, 2002, doi: 10.1063/1.1533112.

[22] S.-H. Jo, H. Yoon, Y.C. Shin, and B.D. Youn, "A graded phononic crystal with decoupled double defects for broadband energy localization," *Int. J. Mech. Sci.*, vol. 183, p. 105833, 2020, doi: 10.1016/j.ijmecsci.2020.105833.

[23] Z. Wen, Y. Jin, P. Gao, X. Zhuang, T. Rabczuk, and B. Djafari-Rouhani, "Topological cavities in phononic plates for robust energy harvesting," *Mech. Syst. Signal Process.*, vol. 162, p. 108047, 2022, doi: 10.1016/j.ymssp.2021.108047.

[24] S.-H. Jo, H. Yoon, Y.C. Shin, and B.D. Youn, "An analytical model of a phononic crystal with a piezoelectric defect for energy harvesting using an electroelastically coupled transfer matrix," *Int. J. Mech. Sci*, vol. 193, p. 106160, 2021, doi: 10.1016/j.ijmecsci.2020.106160.

[25] S. Alagoz, O.A. Kaya, and B.B. Alagoz, "Frequency-controlled wave focusing by a sonic crystal lens," *Appl. Acoust.*, vol. 70, no. 11–12, pp. 1400–1405, 2009, doi: 10.1016/j.apacoust.2009.06.001.

[26] O.R. Bilal and M.I. Hussein, "Ultrawide phononic band gap for combined in-plane and out-of-plane waves," *Phys. Rev. E*, vol. 84, no. 6, p. 065701, 2011, doi: 10.1103/PhysRevE.84.065701.

[27] S. Garus and W. Sochacki, "Structure optimization of quasi one-dimensional acoustic filters with the use of a genetic algorithm," *Wave Motion*, vol. 98, p. 102645, 2020, doi: 10.1016/j.wavemoti.2020.102645.

[28] W. Sochacki, K. Błoch, and S. Garus, "Monuments protection against vibrations and noise using quasi one-dimensional acoustic barriers," *Int. J. Conserv. Sci.*, vol. 10, no. 4, pp. 805–810, 2019.

[29] W. Sochacki *et al.*, "Designing Two-band mechanical wave filters using genetic algorithm," *Acta Phys. Pol. A*, vol. 139, no. 5, pp. 479–482, 2021, doi: 10.12693/APhysPolA.139.479.

[30] S. Garus, W. Sochacki, J. Garus, and A.V. Sandu, "Optimization of a bandgap in the ultrasonic phononic coating," *Arch. Metall. Mater.*, vol. 66, no. 2, pp. 537–542, 2021, doi: 10.24425/amm.2021.135890.

[31] S. Garus and W. Sochacki, "The effect of layer thickness on the reflectance of a quasi one-dimensional composite built with $Zr_{55}Cu_{30}Ni_5Al_{10}$ amorphous alloy and epoxy resin," *Arch. Metall. Mater.*, vol. 66, no. 2, pp. 503–510, 2021, doi: 10.24425/amm.2021.135885.

[32] S. Garus, W. Sochacki, and M. Bold, "Transmission properties of two-dimensional chirped phononic crystal," *Acta Phys. Pol. A*, vol. 135, no. 2, pp. 153–156, 2019, doi: 10.12693/APhysPolA.135.153.

[33] X. Liang, A.C. To, J. Du, and Y.J. Zhang, "Topology optimization of phononic-like structures using experimental material interpolation model for additive manufactured lattice infills," *Comput. Methods Appl. Mech. Eng.*, vol. 377, p. 113717, 2021, doi: 10.1016/j.cma.2021.113717.

6

Bull. Pol. Acad. Sci. Tech. Sci., vol. 71, no. 3, p. e144609, 2023

Influence of spatial distribution and the type of material on the occurrence of bandgaps in phononic crystals

[34] H. Gao, J. Liang, B. Li, C. Zheng, and T. Matsumoto, "A level set based topology optimization for finite unidirectional acoustic phononic structures using boundary element method," *Comput. Methods Appl. Mech. Eng.*, vol. 381, p. 113776, 2021, doi: 10.1016/j.cma.2021.113776.

[35] W. Xu, J. Ning, Z. Lin, W. Qi, H. Liu, and W. Wang, "Multi-objective topology optimization of two-dimensional multi-phase microstructure phononic crystals," *Mater. Today Commun.*, vol. 22, p. 100801, 2020, doi: 10.1016/j.mtcomm.2019.100801.

[36] A.K. Sharma, M. Kosta, G. Shmuel, and O. Amir, "Gradient-based topology optimization of soft dielectrics as tunable phononic crystals," *Composite Struct.*, vol. 280, p. 114846, 2022, doi: 10.1016/j.compstruct.2021.114846.

[37] Y. Chen, J. Li, and J. Zhu, "Topology optimization of quantum spin Hall effect-based second-order phononic topological insulator," *Mech. Syst. Signal Process.*, vol. 164, p. 108243, 2022, doi: 10.1016/j.ymssp.2021.108243.

[38] J.A. Kulpe, K.G. Sabra, and M.J. Leamy, "A three-dimensional Bloch wave expansion to determine external scattering from finite phononic crystals," *J. Acoust. Soc. Am.*, vol. 137, no. 6, pp. 3299–3313, 2015, doi: 10.1121/1.4921548.

[39] L. Luschi and F. Pieri, "A Transmission line model for the calculation of phononic band gaps in perforated mems structures," *Procedia Eng.*, vol. 47, pp. 1101–1104, 2012, doi: 10.1016/j.proeng.2012.09.343.

[40] Y. Jin *et al.*, "Design of vibration isolators by using the Bragg scattering and local resonance band gaps in a layered honeycomb meta-structure," *J. Sound Vib.*, vol. 521, p. 116721, 2022, doi: 10.1016/j.jsv.2021.116721.

[41] A. Mehaney, A.M. Ahmed, F. Segovia-Chaves, and H.A. Elsayed, "Tunability of local resonant modes in Fibonacci one-dimensional phononic crystals by hydrostatic pressure," *Optik*, vol. 244, p. 167546, 2021, doi: 10.1016/j.ijleo.2021.167546.

[42] B. Cai and P.J. Wei, "Band Gaps of 2D Phononic Crystal with Graded Interphase," *Appl. Mech. Mater.*, vol. 121–126, pp. 2567–2571, 2011, doi: 10.4028/www.scientific.net/AMM.121-126.2567.

[43] X. Pu and Z. Shi, "Periodic pile barriers for Rayleigh wave isolation in a poroelastic half-space," *Soil Dyn. Earthq. Eng.*, vol. 121, pp. 75–86, 2019, doi: 10.1016/j.soildyn.2019.02.029.

[44] C. Zhao, J. Zheng, T. Sang, L. Wang, Q. Yi, and P. Wang, "Computational analysis of phononic crystal vibration isolators via FEM coupled with the acoustic black hole effect to attenuate railway-induced vibration," *Constr. Build. Mater.*, vol. 283, p. 122802, 2021, doi: 10.1016/j.conbuildmat.2021.122802.

[45] L. Yao, G. Jiang, F. Wu, and J. Luo, "Band structure computation of two-dimensional and three-dimensional phononic crystals using a finite element-least square point interpolation method," *Appl. Math. Model.*, vol. 76, pp. 591–606, 2019, doi: 10.1016/j.apm.2019.05.052.

[46] F.-L. Li, C. Zhang, and Y.-S. Wang, "Band structure analysis of phononic crystals with imperfect interface layers by the BEM," *Eng. Anal. Bound. Elem.*, vol. 131, pp. 240–257, 2021, doi: 10.1016/j.enganabound.2021.06.024.

[47] Q. Wei, X. Ma, and J. Xiang, "Band structure analysis of two-dimensional photonic crystals using the wavelet-based boundary element method," *Eng. Anal. Bound. Elem.*, vol. 134, pp. 1–10, 2022, doi: 10.1016/j.enganabound.2021.09.025.

[48] A. Rostami, H. Kaatuzian, and B. Rostami-Dogolsara, "Acoustic 1×2 demultiplexer based on fluid-fluid phononic crystal ring resonators," *J. Mol. Liq.*, vol. 308, p. 113144, 2020, doi: 10.1016/j.molliq.2020.113144.

[49] N. Aravantinos-Zafiris, F. Lucklum, and M.M. Sigalas, "Complete phononic band gaps in the 3D Yablonovite structure with spheres," *Ultrasonics*, vol. 110, p. 106265, 2021, doi: 10.1016/j.ultras.2020.106265.

[50] D. Tarrazó-Serrano, S. Castiñeira-Ibáñez, E. Sánchez-Aparisi, A. Uris, and C. Rubio, "MRI compatible planar material acoustic lenses," *Appl. Sci.*, vol. 8, no. 12, p. 2634, Dec. 2018, doi: 10.3390/app8122634.

[51] S. Yang, W.-D. Yu, and N. Pan, "Band structure in two-dimensional fiber–air phononic crystals," *Physica B Condens.*, vol. 406, no. 4, pp. 963–966, 2011, doi: 10.1016/j.physb.2010.12.039.

[52] Y. Wang, W. Song, E. Sun, R. Zhang, and W. Cao, "Tunable passband in one-dimensional phononic crystal containing a piezoelectric $0.62Pb(Mg_{1/3}Nb_{2/3})O_3$–$0.38PbTiO_3$ single crystal defect layer," *Physica E Low Dimens. Syst. Nanostruct.*, vol. 60, pp. 37–41, 2014, doi: 10.1016/j.physe.2014.02.001.